Journal of
Applied Remote Sensing

RemoteSensing.SPIEDigitalLibrary.org

In silico analysis of decomposed reflectances of C3 and C4 plants aiming at the effective assessment of crop needs

Gladimir V. G. Baranoski
Spencer Van Leeuwen
Tenn F. Chen

SPIE.

Gladimir V. G. Baranoski, Spencer Van Leeuwen, Tenn F. Chen, "*In silico* analysis of decomposed reflectances of C3 and C4 plants aiming at the effective assessment of crop needs," *J. Appl. Remote Sens.* **11**(2), 026012 (2017), doi: 10.1117/1.JRS.11.026012.

In silico analysis of decomposed reflectances of C3 and C4 plants aiming at the effective assessment of crop needs

Gladimir V. G. Baranoski,[a,*] Spencer Van Leeuwen,[a] and Tenn F. Chen[b]
[a]University of Waterloo, David R. Cheriton School of Computer Science, Natural Phenomena Simulation Group, Waterloo, Ontario, Canada
[b]Google Inc., Mountain View, California, United States

Abstract. By separating the surface and subsurface components of foliar hyperspectral signatures using polarization optics, it is possible to enhance the remote discrimination of different plant species and optimize the assessment of different factors associated with their health status. These initiatives, in turn, can lead to higher crop yield and lower environmental impact. It is important to consider, however, that the main varieties of crops, represented by C3 (e.g., soy) and C4 (e.g., maize) plants, have markedly distinct morphological characteristics. Accordingly, the influence of these characteristics on their interactions with impinging light may affect the selection of optimal probe wavelengths for specific applications making use of combined hyperspectral and polarization measurements. In this paper, we compare the sensitivity of the total (including surface and subsurface components) and subsurface reflectance responses of C3 and C4 plants to different spectral and geometrical light incidence conditions. This investigation is supported by measured biophysical data and predictive light transport simulations. The results of our comparisons indicate that the total and subsurface reflectance responses of C3 and C4 plants depict well-defined patterns of sensitivity for varying illumination conditions. We believe that these patterns should be considered in the design of high-fidelity crop discrimination and monitoring procedures. [DOI: 10.1117/1.JRS.11.026012]

Keywords: foliar optical properties; surface reflectance; subsurface reflectance; polarization; simulation.

Paper 16890 received Nov. 19, 2016; accepted for publication Apr. 17, 2017; published online May 2, 2017.

1 Introduction

Plants are considered primary remote sensing targets due to their importance to sustain human and animal life. Not surprisingly, there has been a vast body of work devoted to the acquisition and analysis of plants' spectral data as well as to the modeling of their interactions with light at different scales, from individual leaves and canopies to entire landscapes covered by vegetation.[1] For the success of these applications, it is essential that stress factors, such as water and nutrient losses, can be effectively detected and timely addressed. These factors can result in changes in how plants absorb, transmit, and reflect light. Accordingly, the spectral signatures of their leaves can be used as physiological-status indicators and assist in the mitigation of the adverse effects triggered by the stress factors. These connections provide the basis for the increasing use of hyperspectral technology in the remote sensing of crops.[2–4]

Stress factors affecting the physiological status of plants tend to have a dominant impact on the subsurface (diffuse) component of their reflectance since the surface (specular) component represents light that does not penetrate their foliar tissues. Using hyperspectral devices combined with polarization optics, one can perform examinations of changes in foliar subsurface reflectance,[5,6] which, in turn, can potentially lead to more precise stress assessments. However,

*Address all correspondence to: Gladimir V. G. Baranoski, E-mail: gvgbaran@cs.uwaterloo.ca

it is important to consider that the main varieties of cultivated plants belonging to the C3 and C4 groups have distinct morphological characteristics that can affect their hyperspectral responses.[7]

In this paper, which is an updated and extended version of a conference presentation,[8] we investigate the sensitivity of C3 and C4 plants' total reflectance (including surface and subsurface components) and subsurface reflectance to different illumination conditions. More specifically, we consider two species representative of these groups, namely soy (*Soja hispida*, also referred to as *Glycine max* L.) and maize (*Zea mays* L., commonly known as corn), respectively. While the former is characterized by bifacial leaves, the latter is characterized by unifacial leaves. We note, however, that there are C3 species characterized by unifacial leaves[9] and C4 species characterized by bifacial leaves.[10] Our investigation is based on *in silico* experiments in which we simulated light interactions with different leaf specimens representative of these two species. In these experiments, the specific morphological characteristics of soy and maize leaves were taken into account. Comparing the simulation results obtained for these two species, one can observe trends that should be taken into consideration by initiatives aimed at the interpretation of the plants' hyperspectral responses. We remark that the higher the reliability of these interpretations, the higher the fidelity of procedures for the discrimination and monitoring of crops using remote sensing technology.

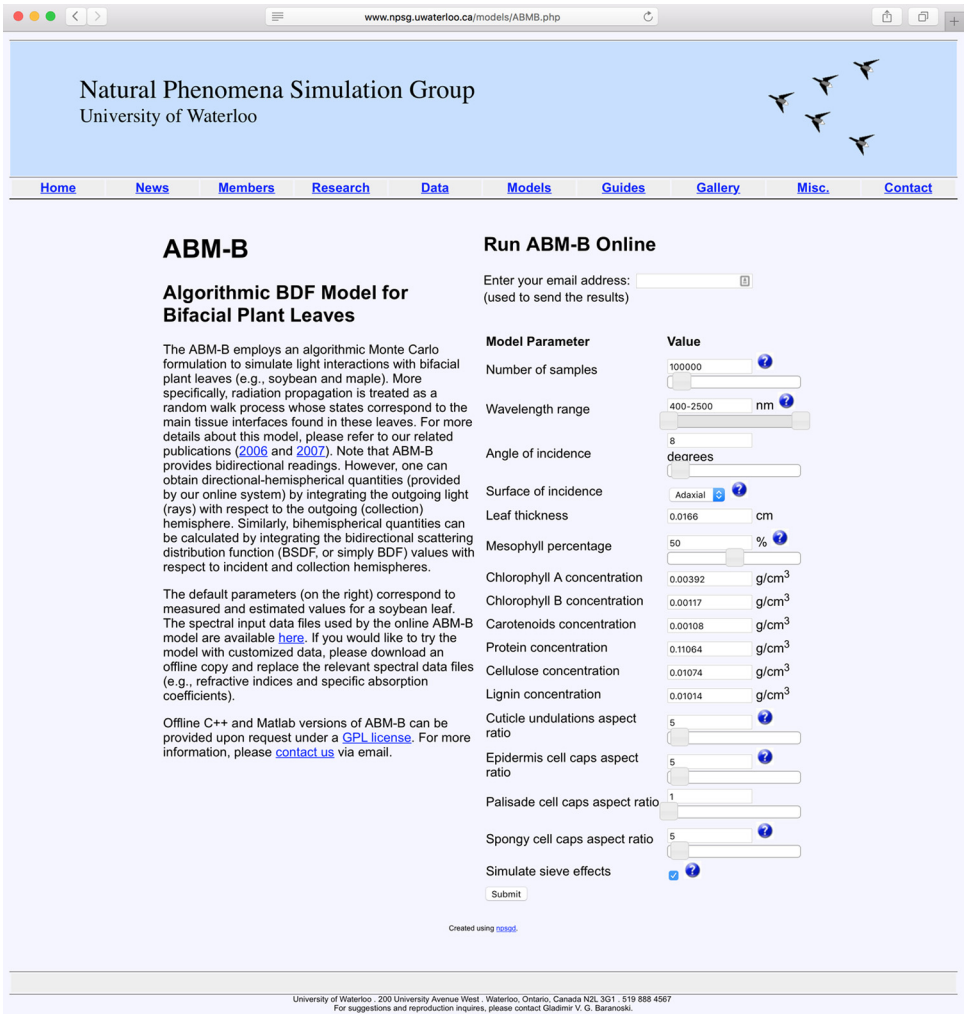

Fig. 1 The web interface for the ABM-B model[15] available through the Natural Phenomena Simulation Group Distributed (NPSGD) system.[17] Through this interface, researchers can configure biophysical parameters and execute light transport simulations involving plants characterized by bifacial leaves.

2 Materials and Methods

2.1 *Simulation Framework Overview*

Our *in silico* experiments were performed using predictive hyperspectral models of light interaction with bifacial and unifacial plant leaves, namely algorithmic bidirectional scattering distribution function (BDF) model for bifacial (ABM-B) plant leaves and algorithmic BDF model for unifacial (ABM-U) plant leaves, respectively.[11,12] It is important to note that these models have been extensively evaluated through quantitative and qualitative comparisons of modeled results with actual measured data.[11,13,14] To allow the reproduction and extension of our investigation to other experimental conditions, we made these models and the supporting biophysical data (e.g., refractive indices and absorption coefficients) employed in this work accessible through an online system.[15,16] Using this system,[17] researchers can configure simulation parameters (e.g., wavelength range and angle of incidence) as well as specimen characterization data (e.g., thickness and pigment contents) through web interfaces (Figs. 1 and 2) and run the models. For the characterization of typical exemplars of soy and maize leaves, we used measured data[18] and observations reported in the literature.[11,13,14] In Table 1, we provide a summary of the values assigned to these specimens' biophysical parameters during this investigation. Note that we refer to the soy specimens as S1 and S2 and the maize specimens as M1 and M2.

Within the ABM-B and ABM-U ray-optics formulations, a ray interacting with a given leaf specimen can be associated with any selected wavelength within spectral regions of interest in

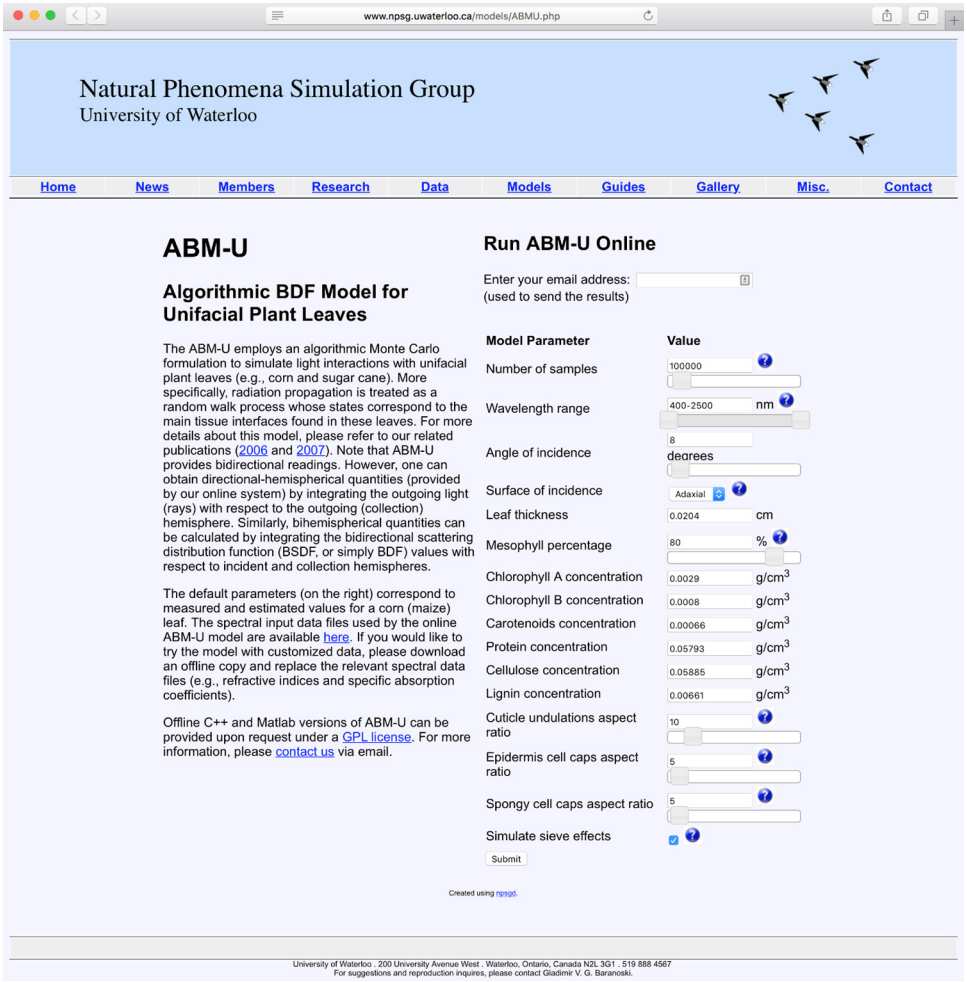

Fig. 2 The web interface for the ABM-U model[16] available through the NPSGD system.[17] Through this interface, researchers can configure biophysical parameters and execute light transport simulations involving plants characterized by unifacial leaves.

Table 1 Parameters employed in the characterization of the soy (S1 and S2) and maize (M1 and M2) specimens. The thickness values and biochemical data assigned to S1, S2, M1, and M2 correspond to the actual characteristics of the soy and maize specimens used to obtain the LOPEX[18] spectral measurements 219, 225, 141, and 537, respectively. It is worth noting that the thickness values and biochemical data provided in LOPEX were obtained from leaf specimens collected during the period of maximum phonological activity of the sampled plants.

Parameter	S1	S2	M1	M2
Thickness (cm)	0.01660	0.0106	0.0204	0.0224
Mesophyll percentage (%)	50	50	80	80
Chlorophyll A concentration (g/cm^3)	0.00392	0.00605	0.00290	0.00342
Chlorophyll B concentration (g/cm^3)	0.00117	0.00170	0.00080	0.00120
Carotenoids concentration (g/cm^3)	0.00108	0.00167	0.00066	0.00091
Protein concentration (g/cm^3)	0.11064	0.14752	0.05793	0.06656
Cellulose concentration (g/cm^3)	0.01074	0.07900	0.05804	0.07152
Lignin concentration (g/cm^3)	0.01014	0.01361	0.00661	0.00760
Cuticle undulations aspect ratio	5	5	10	10
Epidermal cell caps aspect ratio	5	5	5	5
Palisade cell caps ratio	1	1	—	—
Spongy cell caps aspect ratio	5	5	5	5

the visible and near-infrared (NIR) domains. Hence, these models can provide reflectance readings with different spectral resolutions. In terms of illumination and collection geometries, these models can provide bidirectional reflectance and transmittance quantities by recording the direction of the outgoing rays using a virtual gonioreflectometer.[19,20] In addition, one can obtain directional-hemispherical reflectance and transmittance quantities by integrating the outgoing rays with respect to the collection hemisphere using a virtual spectrophotometer.[20,21] The modeled curves depicted in this work correspond to directional-hemispherical reflectances obtained from the leaves' adaxial surfaces. In their computation, we considered a spectral resolution of 5 nm and employed 10^6 sample rays per wavelength.

2.2 *Sensitivity Analysis*

In our experiments, distinct illumination conditions were simulated by varying the wavelength of the impinging light and the angle of incidence, which is denoted by θ and specified with respect to the specimen's normal. To compare the total reflectance and subsurface reflectance of the selected specimens under these conditions, we performed a parameter differential sensitivity analysis,[22,23] also known as direct sensitivity analysis method. It consists of the computation of the sensitivity index (SI) originally introduced by Hoffman and Gardner[24] to account for uncertainties in environmental assessment models. It provides the ratio of the change in the output to the variation in the selected parameter while all other parameters remain fixed. An SI equal to 1.0 indicates complete sensitivity (or maximum impact), while an SI less than 0.01 indicates that the output is insensitive to variations in the parameter.[24]

In our work, the SI is used to provide the ratio of the change in reflectance to the variation in the angle of incidence, and it is expressed as

$$\mathrm{SI} = \frac{|\rho_0(\lambda_i) - \rho_\theta(\lambda_i)|}{\max\{\rho_0(\lambda_i), \rho_\theta(\lambda_i)\}}, \tag{1}$$

where ρ_0 corresponds to a baseline reflectance curve computed considering $\theta = 0$ deg and ρ_θ represents a reflectance curve computed considering a specific value assigned to θ.

Since the SI refers to pairs of data points, we computed the mean sensitivity index (MSI) for the spectral regions of interest, namely visible (400 to 700 nm), NIR-A (700 to 1300 nm), and NIR-B (1300 to 2500 nm), to assess the mean ratio of the change in reflectance to the variation in the angle of incidence. This index is expressed as

$$\mathrm{MSI} = \frac{1}{N}\sum_{i=1}^{N}\frac{|\rho_0(\lambda_i) - \rho_\theta(\lambda_i)|}{\max\{\rho_0(\lambda_i), \rho_\theta(\lambda_i)\}}, \tag{2}$$

where N is the total number of wavelengths sampled with a 5-nm resolution within a selected spectral region.

When comparing a pair of reflectance curves obtained considering two different angles of incidence, one can assess the impact of this angular variation in absolute or relative terms. For example, by visually inspecting the two sets of curves as shown in Fig. 3, one can verify that an angular variation from 0 deg to 60 deg results in larger absolute differences $[|\rho_0(\lambda_i) - \rho_\theta(\lambda_i)|]$ among the total reflectance curves than among the subsurface reflectance curves [Fig. 4(a)]. However, when one examines the SI values computed for these two sets of curves [Fig. 4(b)], one can verify that in relative terms the angular variation from 0 deg to 60 deg has a larger impact on portions of the subsurface reflectance curves. It is important to note that MSI, differently from other metrics, such as root-mean-square error, is associated with the relative differences among data points instead of the absolute differences among these points. Hence, our use of the MSI metrics in this investigation can be seen as a qualitative complement to the quantitative comparisons among reflectance curves obtained considering different angles of incidence.

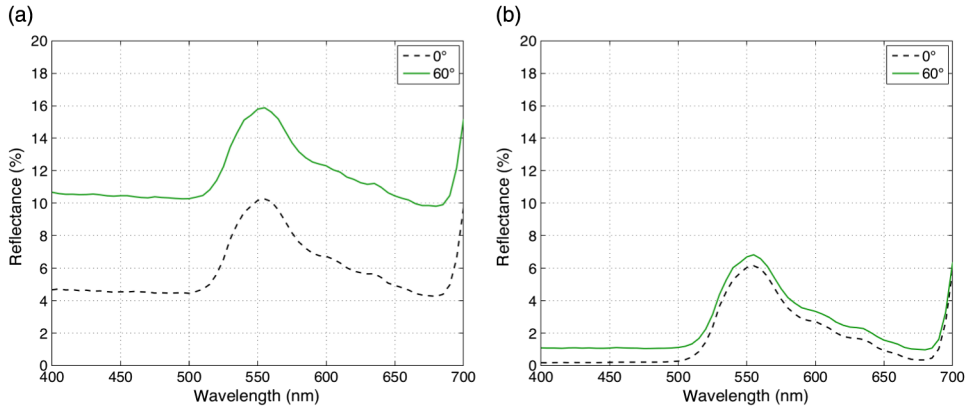

Fig. 3 (a) Total reflectance and (b) subsurface reflectance curves computed for the soy specimen S1 considering two angles of incidence: 0 deg and 60 deg. The curves were obtained using the ABM-B model[15] and the data provided in Table 1.

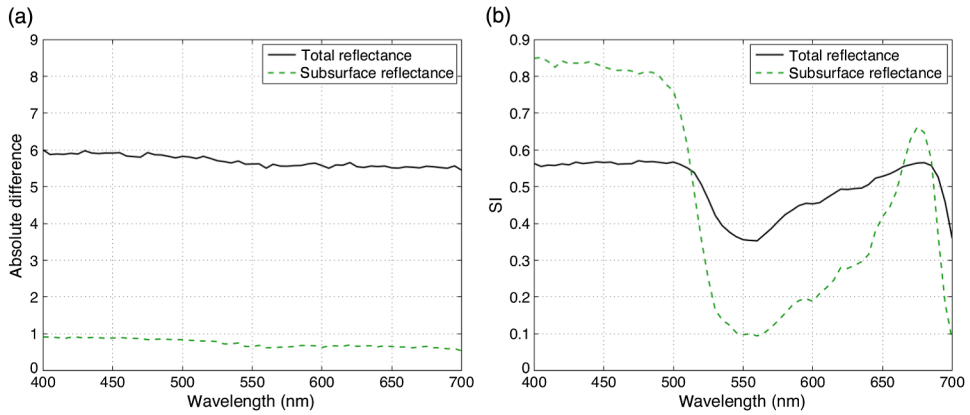

Fig. 4 (a) Absolute difference and (b) SI values computed for the total reflectance and subsurface reflectance curves depicted in Fig. 3.

3 Results and Discussion

The results of our experiments for the soy and maize specimens are presented in Figs. 5 and 6, respectively. As expected, as we increase the angle of incidence from 0 deg to 60 deg, the total reflectance increases for both groups of specimens due to the stronger contribution of the surface component. Within this angular range, it can also be observed that the variations on subsurface reflectance were substantially less pronounced than the corresponding variations in total reflectance.

Although these aspects seem to indicate that the selected bifacial C3 and unifacial C4 specimens present the same behavior with respect to the dependence of their total reflectance and subsurface reflectance on the angle of incidence, a closer examination of their hyperspectral responses across the visible, NIR-A, and NIR-B spectral regions, supported by the computation of the corresponding MSI values within these regions, reveals distinct qualitative trends. As it can be verified in the MSI values provided in Fig. 7, while the sensitivity of the bifacial C3

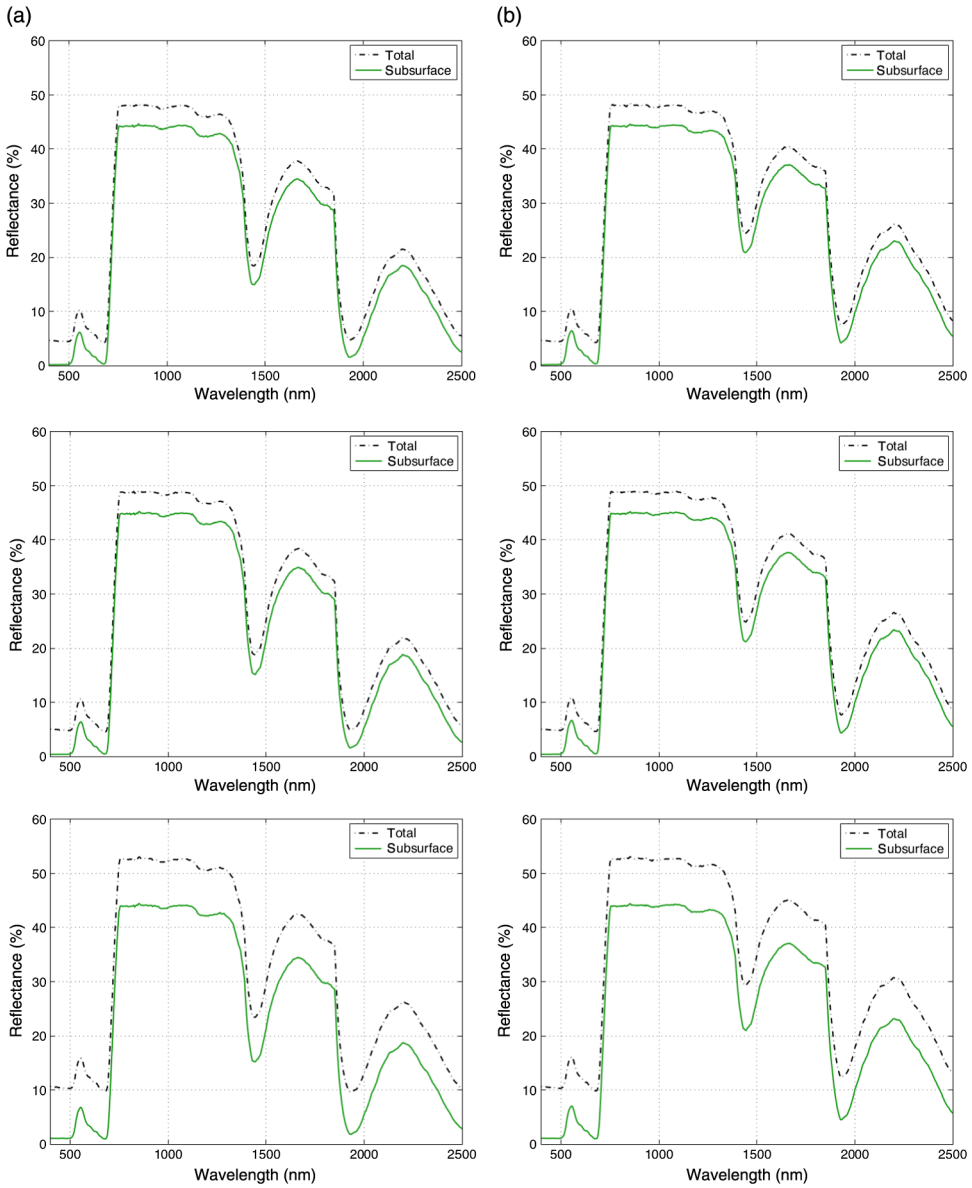

Fig. 5 Total reflectance (surface and subsurface components) and subsurface reflectance curves computed for the soy specimens (a) S1 and (b) S2 considering three angles of incidence: 0 deg (top row), 30 deg (middle row), and 60 deg (bottom row). The curves were obtained using the ABM-B model[15] and the data provided in Table 1.

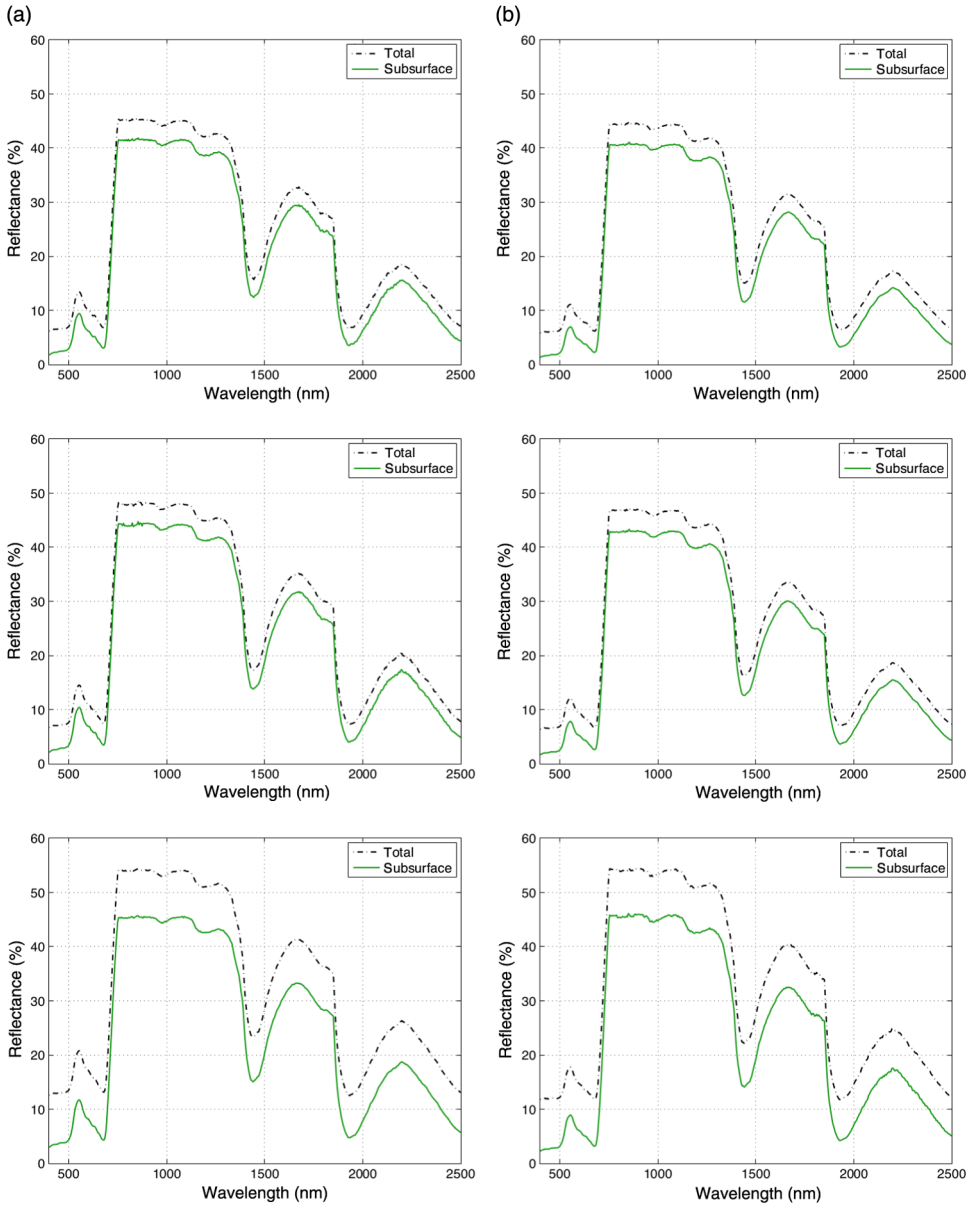

Fig. 6 Total reflectance (surface and subsurface components) and subsurface reflectance curves computed for the maize specimens (a) M1 and (b) M2 considering three angles of incidence: 0 deg (top row), 30 deg (middle row), and 60 deg (bottom row). The curves were obtained using the ABM-U model[16] and the data provided in Table 1.

specimens' total reflectance to variations in the angle of incidence is markedly dominant in the visible region, the sensitivity of the unifacial C4 specimens' total reflectance is more balanced across the three spectral regions of interest. These observations also apply to the selected specimens' subsurface reflectance as indicated by the MSI values provided in Fig. 8.

The MSI values provided in Figs. 7 and 8 also reveal distinct magnitude trends for the selected specimens. More specifically, the sensitivity of the bifacial C3 specimens' subsurface reflectance is more dominant in the visible region than the sensitivity of their total reflectance in the same region. For example, while the ratios of visible to NIR-B MSI values computed for the bifacial C3 specimens' total reflectance are equal to 2.75 (for S1) and 3.35 (for S2) considering an angle of incidence equal to 45 deg, the corresponding ratios for the bifacial C3 specimens' subsurface reflectance are equal to 11.74 (for S1) and 13.87 (for S2). On the other hand, as it was verified with respect to the sensitivity of the unifacial C4 specimens' total reflectance, the sensitivity of their subsurface reflectance is more balanced across the three spectral regions of

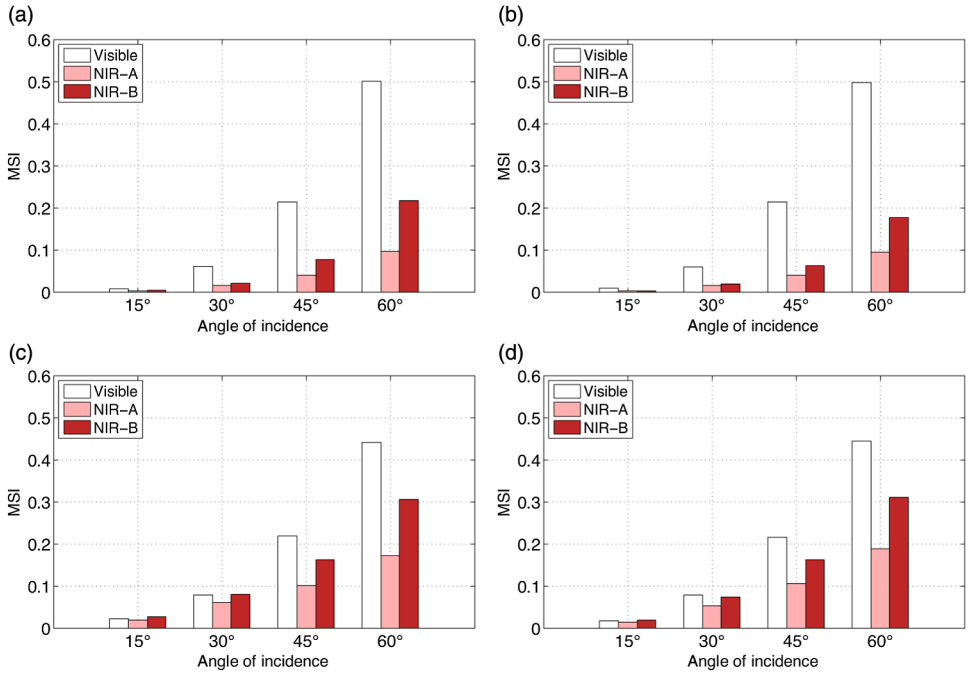

Fig. 7 MSI values calculated for the total reflectance of the soy (top row) and maize (bottom row) specimens (obtained considering four angles of incidence: 15 deg, 30 deg, 45 deg, and 60 deg) with respect to their total reflectance curve obtained considering normal incidence (0 deg). The curves for the soy and maize specimens were computed using the ABM-B[15] and ABM-U[16] models, respectively. The characterization data employed for the soy specimens (a) S1 and (b) S2 as well as for the maize specimens (c) M1 and (d) M2 are provided in Table 1.

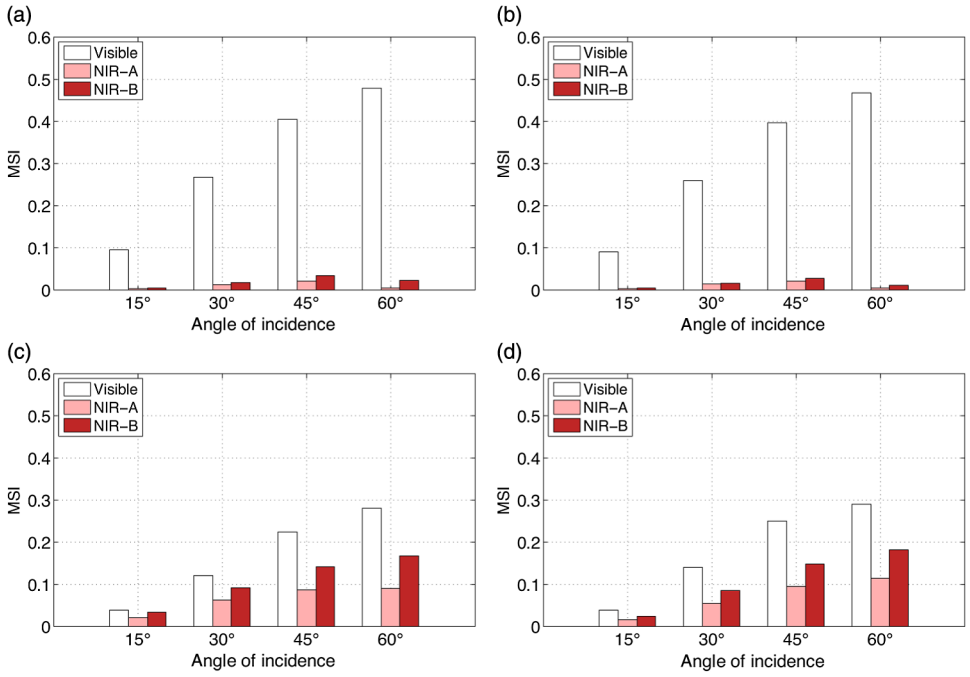

Fig. 8 MSI values calculated for the subsurface reflectance of the soy (top row) and maize (bottom row) specimens (obtained considering four angles of incidence: 15 deg, 30 deg, 45 deg, and 60 deg) with respect to their subsurface reflectance curve obtained considering normal incidence (0 deg). The curves for the soy and maize specimens were computed using the ABM-B[15] and ABM-U[16] models, respectively. The characterization data employed for the soy specimens (a) S1 and (b) S2 as well as for the maize specimens (c) M1 and (d) M2 are provided in Table 1.

interest. For example, the ratios of visible to NIR-B MSI values computed for the unifacial C4 specimens' total reflectance are equal to 1.34 (for M1) and 1.57 (for M2) considering an angle of incidence equal to 45 deg. Similarly, the corresponding ratios for the unifacial C4 specimens' subsurface reflectance are equal to 1.31 (for M1) and 1.67 (for M2). We note that these magnitude trends are also observed with respect to the other angles of incidence considered in this investigation.

Clearly, the success of remote sensing applications involving the discrimination and monitoring of crops depends on the correct understanding about the optical properties of the target species. Such an understanding, in turn, is derived from theoretical and applied investigations supported by measured foliar spectral data. These data are often obtained at low angles of incidence, with angles between 2.5 deg and 15 deg being commonly employed in investigations reported in the literature.[14,18,25–28] To aggregate the results of these investigations in a meaningful manner, it is necessary to examine whether these angular variations may have a significant impact on the measured spectral quantities and how this impact may vary for the two main groups of cultivated species.

While variations in the angle of incidence up to 15 deg had a minor impact (close to or below the insensitivity threshold of 0.01) on the selected bifacial C3 specimens' total reflectance (Table 2), they had a more noticeable impact on the selected unifacial C4 specimens' total reflectance (Table 3). These aspects are further illustrated by the reflectance plots as shown in Fig. 9. In addition, these variations had also a minor impact on the selected bifacial C3 specimens' subsurface reflectance for measurements performed in the NIR-A and NIR-B regions (Table 2). However, the same cannot be claimed for the selected unifacial C4 specimens (Table 3). These distinct sensitivity behaviors are also further illustrated by the reflectance plots as shown in Fig. 10.

These observations suggest that, for readings obtained considering an angle of incidence below 15 deg, angular variations tend to have a larger impact on the spectral responses of unifacial C4 specimens. Although this impact may not seem substantial when one visually inspects curves considering a relatively large spectral region (e.g., Figs. 9 and 10), close examinations of the resulting reflectance changes within specific spectral domains show that these changes may be significant when compared to the corresponding changes observed in the responses of bifacial C3 specimens. This aspect is illustrated by the plots presented in Fig. 11. Accordingly, these distinct sensitivities to angular variations should be taken into account during investigations based on the measurement of subtle changes on foliar spectral responses.

Finally, we remark that, despite the significant morphological differences between bifacial C3 and unifacial C4 specimens, these plants share a similar dependence on the light absorbers

Table 2 MSI values associated with the bifacial C3 specimens' total and subsurface reflectance curves obtained considering an angle of incidence of 15 deg.

	Total reflectance			Subsurface reflectance		
Specimens	Visible	NIR-A	NIR-B	Visible	NIR-A	NIR-B
S1	0.0095	0.0038	0.0047	0.0952	0.0041	0.0054
S2	0.0112	0.0040	0.0046	0.0903	0.0041	0.0049

Table 3 MSI values associated with the unifacial C4 specimens' total and subsurface reflectance curves obtained considering an angle of incidence of 15 deg.

	Total reflectance			Subsurface reflectance		
Specimens	Visible	NIR-A	NIR-B	Visible	NIR-A	NIR-B
M1	0.0236	0.0206	0.0279	0.0397	0.0223	0.0342
M2	0.0179	0.0149	0.0200	0.0401	0.0164	0.0255

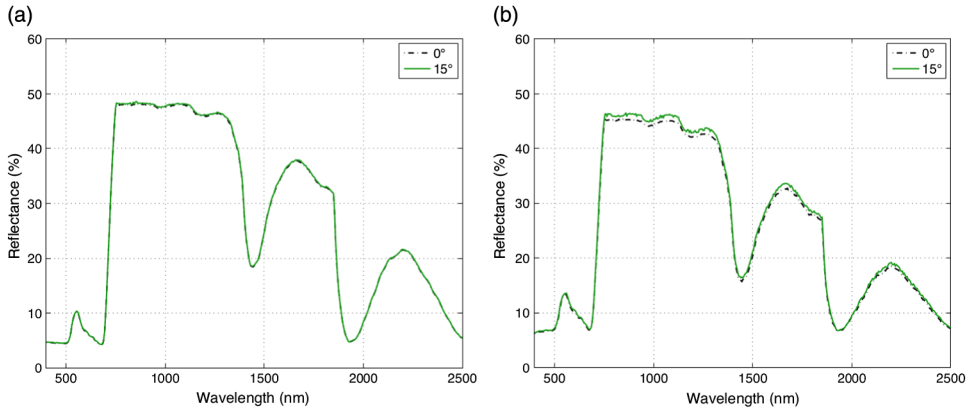

Fig. 9 Total reflectance curves computed for specimens (a) S1 and (b) M1 considering two angles of incidence. The curves were obtained using the ABM-B and ABM-U models[15] and the data provided in Table 1.

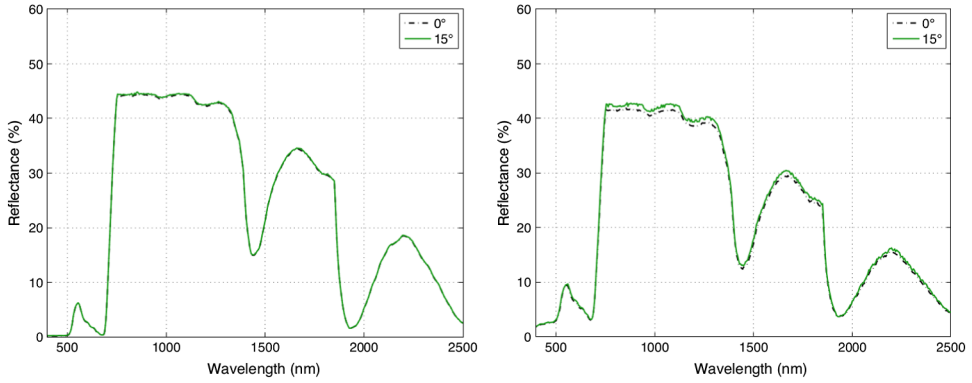

Fig. 10 Subsurface reflectance curves computed for specimens (a) S1 and (b) M1 considering two angles of incidence. The curves were obtained using the ABM-B and ABM-U models[15] and the data provided in Table 1.

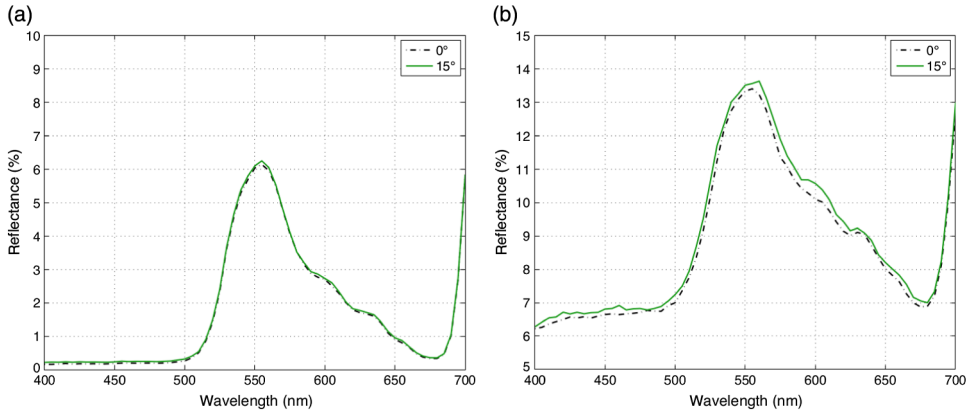

Fig. 11 Zoom-in of total subsurface reflectance curves computed for specimens (a) S1 and (b) M1 in the visible domain and considering two angles of incidence. The curves were obtained using the ABM-B and ABM-U models[15] and the data provided in Table 1.

present in their foliar tissues. For example, while their visible and NIR-B spectral responses are significantly affected by the presence of chlorophyll and water, respectively, their NIR-A spectral responses are not characterized by a similar dependence.[20] Accordingly, NIR-A responses are relatively less susceptible to angular variations affecting the path of light interacting with these

materials. This aspect is reflected on the lower MSI values computed for NIR-A responses in comparison with the corresponding MSI values computed for visible and NIR-B responses. However, as indicated by the MSI values shown in Figs. 7 and 8 as well as in Tables 2 and 3, changes in NIR-A reflectance due to variations on the angle of incidence tend to be more significant for unifacial C4 specimens than for bifacial C3 specimens, even for relatively small angles of incidence (up to 15 deg) as it can be also observed in the plots presented in Figs. 9 and 10.

4 Conclusion

The *in silico* experiments described are by no means exhaustive, and any generalization regarding their outcomes may be premature. Nonetheless, our findings suggest that procedures devised to obtain information about plants' physiological status based on their hyperspectral responses should be flexible enough to account for the distinct morphological characteristics of plants belonging to C3 and C4 groups. Otherwise, the same procedure or apparatus capable of providing high-fidelity results for a plant belonging to one group may lead to unreliable interpretations for a plant belonging to the other.

The effectiveness of indicators of plants' physiological status, such as the subsurface reflectance to transmittance ratio employed by Vanderbilt et al.,[6] depends on how these quantities are obtained, especially when multiple measurements are performed for different specimens. In these cases, small angular variations may introduce errors in the computation of these indicators. Our findings also suggest that, for measurements performed at more conspicuous low angles of incidence [specified with respect to the specimen's normal (Sec. 2.2)], the magnitude of these errors can be higher for unifacial C4 specimens than for bifacial C3 specimens. As future work, we plan to expand our *in silico* experiments to other representative species belonging to the C3 and C4 groups, and to investigate aspects involving the spatial distribution of the light propagated by these plants.

Acknowledgments

This work was supported by the Natural Sciences and Engineering Research Council of Canada (NSERC-Discovery Grant No. 237337).

References

1. M. Disney, "Remote sensing of vegetation: potentials, limitations, developments and applications," in *Canopy Photosynthesis: From Basics to Applications*, K. Hikosaka, U. Niinemets, and N. Anten, Eds., pp. 289–232, Springer, Dordrecht (2016).
2. K. Uto and Y. Kosugi, "Hyperspectral manipulation for the water stress evaluation of plants," *Contemp. Mater.* **1**(3), 18–25 (2012).
3. P. Zarco-Tejada et al., "Vegetation stress detection through chlorophyll a + b estimation and fluorescence effects on hyperspectral imagery," *J. Environ. Qual.* **31**, 1433–1441 (2002).
4. J. Verrelst et al., "Optical remote sensing and the retrieval of terrestrial vegetation bio-geophysical properties–a review," *ISPRS J. Photogramm. Remote Sens.* **108**, 273–290 (2015).
5. V. Vanderbilt, L. Grant, and S. Ustin, "Polarization of light by vegetation," in *Photon-Vegetation Interactions: Applications in Optical Remote Sensing and Ecology*, R. Nynemi and J. Ross, Eds., pp. 191–228, Springer Verlag, Berlin, Germany (1991).
6. V. Vanderbilt, C. Daughtry, and R. Dahlgren, "Relative water content, bidirectional reflectance and bidirectional transmittance of the interior of detached leaves during dry down," in *IEEE Int. Geoscience & Remote Sensing Symp. (IGARSS'15)* (2015).
7. G. Baranoski et al., "On the high-fidelity monitoring of C3 and C4 crops under nutrient and water stress," *Proc. SPIE* **8524**, 85240W (2012).
8. G. Baranoski, S. Van Leeuwen, and T. Chen, "On the decomposition of foliar hyperspectral signatures for the high-fidelity discrimination and monitoring of crops," *Proc. SPIE* **9880**, 98800G (2016).

9. R. Muhaidat et al., "Characterization of C3-C4 intermediate species in the genus Heliotropium L. (Boraginaceae): anatomy, ultrastructure and enzyme activity," *Plant Cell Environ.* **34**, 1723–1736 (2011).
10. H. Akhani et al., "Occurrence and forms of Kranz anatomy in photosynthetic organs and characterization of NAD-ME subtype C4 photosynthesis in Blepharis ciliaris (L.) B. L. Burtt (Acanthaceae)," *J. Exp. Bot.* **59**(7), 1755–1765 (2008).
11. G. Baranoski, "Modeling the interaction of infrared radiation (750 to 2500 nm) with bifacial and unifacial plant leaves," *Remote Sens. Environ.* **100**, 335–347 (2006).
12. G. Baranoski and D. Eng, "An investigation on sieve and detour effects affecting the interaction of collimated and diffuse infrared radiation (750 to 2500 nm) with plant leaves," *IEEE Trans. Geosci. Remote Sens.* **45**, 2593–2599 (2007).
13. D. Eng and G. Baranoski, "The application of photoacoustic absorption spectral data to the modeling of leaf optical properties in the visible range," *IEEE Trans. Geosci. Remote Sens.* **45**, 4077–4086 (2007).
14. G. Baranoski et al., "In silico assessment of environmental factors affecting the spectral signature of C4 plants in the visible domain," *Int. J. Remote Sens.* **33**(4), 1190–1213 (2012).
15. NPSG, "Run ABM-B online," Natural Phenomena Simulation Group, University of Waterloo, Canada, 2011, http://www.npsg.uwaterloo.ca/models/ABMB.php.
16. NPSG, "Run ABM-U online," Natural Phenomena Simulation Group, University of Waterloo, Canada, 2011).http://www.npsg.uwaterloo.ca/models/ABMU.php.
17. G. Baranoski et al., "Rapid dissemination of light transport models on the web," *IEEE Comput. Graphics Appl.* **32**(3), 10–15 (2012).
18. B. Hosgood et al., "Leaf optical properties experiment 93," Tech. Rep. Report EUR 16095 EN, Joint Research Center, European Commission, Institute for Remote Sensing Applications, Luxembourg (1995).
19. A. Krishnaswamy and G. Baranoski, "A biophysically-based spectral model of light interaction with human skin," *Comput. Graphics Forum* **23**(3), 331–340 (2004).
20. G. Baranoski and J. Rokne, *Light Interaction With Plants: A Computer Graphics Perspective*, Horwood Publishing, Chichester, United Kingdom (2004).
21. G. Baranoski, J. Rokne, and G. Xu, "Virtual spectrophotometric measurements for biologically and physically-based rendering," *Visual Comput.* **17**(8), 506–518 (2001).
22. D. Hamby, "A review of techniques for parameter sensitivity analysis of environmental models," *Environ. Monit. Assess.* **32**, 135–154 (1994).
23. D. Hamby, "A comparison of sensitivity analysis techniques," *Health Phys.* **68**, 195–204 (1995).
24. F. Hoffman and R. Gardner, "Evaluation of uncertainties in radiological assessment models," Chapter 11 in *Radiological Assessment A Textbook on Environmental Dose Analysis*, J. Till and H. Meyer, Eds., NRC FIN B0766, pp. 1–55, Division of Systems Integration, Office of Nuclear Reactor Regulation, U.S. Nuclear Regulatory Commission, Washington DC (1983).
25. J. Thomas et al., "Estimating leaf water content by reflectance measurements," *Agron. J.* **63**, 845–847 (1971).
26. J. Woolley, "Reflectance and transmittance of light by leaves," *Plant Physiol.* **47**, 656–662 (1971).
27. A. Al-Abbas et al., "Spectra of normal and nutrient-deficient maize leaves," *Agron. J.* **66**, 16–20 (1974).
28. G. Maracci et al., "Interpretation of reflectance spectra by plant physiological parameters," in *Int. Geoscience and Remote Sensing Symp., Remote Sensing: Global Monitoring for Earth Management (IGARSS'91)*, Espoo, Finland, pp. 2303–2306 (1991).

Gladimir V. G. Baranoski obtained his PhD in computer science from the University of Calgary, Canada, in 1998. Currently, he is a faculty member of the David R. Cheriton School of Computer Science at the University of Waterloo, Canada, where he has established the Natural Phenomena Simulation Group. His research interests include primarily the predictive simulation of light interactions with natural materials aimed at interdisciplinary applications. He is a member of SPIE.

Spencer Van Leeuwen is currently pursuing his master of mathematics in computer science at the David R. Cheriton School of Computer Science, the University of Waterloo, Canada. He holds a bachelor of mathematics in computer science and combinatorics and optimization with a minor in music from the same institution. He is also a member of the Natural Phenomena Simulation Group at the University of Waterloo.

Tenn F. Chen received his PhD in computer science from the University of Waterloo in 2016. While there he conducted research related to material appearance with a focus on human skin and relevant temporal phenomena. He is currently working on technologies related to virtual reality at Google Inc. He is a former member and currently a collaborator of the Natural Phenomena Simulation Group at the University of Waterloo.